Research Square

Preprints are preliminary reports that have not undergone peer review.
They should not be considered conclusive, used to inform clinical practice,
or referenced by the media as validated information.

Protective effect of somatostatin on the intestinal epithelial glycocalyx in septic rats: A multi-omics screening study

Jiading Xia
Hebei Medical University
Zhilong Ma
Affiliated Hospital of Chengde Medical University
Jinxin Pan
Affiliated Hospital of Chengde Medical University
Kun Zhang
Affiliated Hospital of Chengde Medical University
Xinran Yu
Affiliated Hospital of Chengde Medical University
Quansheng Du
duquansheng@hebmu.edu.cn

Hebei Medical University

Research Article

Keywords: sepsis, intestinal epithelial glycocalyx, somatostatin, multi-omics, transcriptomics, proteomics

Posted Date: August 24th, 2026

DOI: https://doi.org/10.21203/rs.3.rs-10634306/v1

License: This work is licensed under a Creative Commons Attribution 4.0 International License.
Read Full License

Additional Declarations: No competing interests reported.

Protective effect of somatostatin on the intestinal epithelial glycocalyx in septic rats: A multi-omics screening study

Author information

Jiading Xia[1-3], Zhilong Ma[3], Jinxin Pan[3], Kun Zhang[3], Xinran Yu[3], Quansheng Du[1,2,4*]

1 Department of Critical Care Medicine, Hebei Medical University, Shijiazhuang 050017, Hebei, China

2 Department of Emergency Medicine and Critical Care Medicine (Ward 2), Hebei General Hospital, Shijiazhuang 050051, Hebei, China

3 Department of Critical Care Medicine, Affiliated Hospital of Chengde Medical University, Chengde 067000, Hebei, China

4 Hebei Key Laboratory of Clinical Pharmacy, Shijiazhuang 050051, Hebei, China

*Corresponding author: Quansheng Du, E-mail:duquansheng@hebmu.edu.cn

Abstract

Background: Somatostatin (SST) exerts anti-inflammatory and cytoprotective properties, but its effects on the intestinal epithelial glycocalyx in sepsis and the underlying molecular profiles remain incompletely understood. This study aimed to investigate the protective effect of SST on sepsis-induced intestinal epithelial glycocalyx injury and screen associated candidate molecules via integrated multi-omics analysis.

Methods: A rat sepsis model was established via cecal ligation and puncture (CLP) and treated with SST. Intestinal pathological damage, TNF-α expression and Syndecan-1 levels were assessed by ELISA, HE staining, immunofluorescence and Western blotting. Integrated transcriptomic and

proteomic analyses were performed to screen candidate pathways and molecules, which were further verified by RT-qPCR and Western blotting.

Results: Sepsis induced intestinal mucosal injury, increased TNF-α expression and reduced Syndecan-1 levels. SST administration alleviated intestinal pathological damage, suppressed inflammatory responses and partially restored Syndecan-1 expression. The PPAR signaling pathway was significantly enriched in both omics datasets, and ALDH1L1 and FGFBP1 were identified as differentially expressed candidate molecules restored by SST.

Conclusions: SST may alleviate sepsis-induced intestinal epithelial glycocalyx damage and inhibit inflammation. The candidate pathway and molecules identified by multi-omics provide a basis for further mechanistic research.

Keywords: sepsis; intestinal epithelial glycocalyx; somatostatin; multi-omics; transcriptomics; proteomics

1. Introduction

Sepsis is a life-threatening condition characterised by a dysregulated host response to infection leading to organ dysfunction, representing a major clinical challenge in critical care medicine that urgently requires effective solutions (1).Despite continuous advances in early bundle-based treatment and organ support technologies, specific interventions targeting core pathological mechanisms are still lacking. Consequently, the prevention and reversal of sepsis-associated multiple organ dysfunction syndrome are limited, making it difficult to effectively halt disease progression. As a result, sepsis remains one of the leading causes of death in intensive care units, and optimising precision treatment to improve patient outcomes remains a

core task in critical care medicine (2).

Gastrointestinal dysfunction is a key research focus in sepsis. Its status not only directly affects patients' nutritional intake and recovery but also influences systemic multi-organ function via the gut-organ axis. An intact intestinal mucosal barrier acts as a crucial line of defence against bacterial and endotoxin invasion, effectively preventing harmful substances in the gut from entering the circulation.Preserving intestinal mucosal barrier integrity and blocking gut-mediated inflammatory amplification pathways are key targets for halting sepsis progression and improving patient outcomes (3,4). However, the structure and regulatory network of the intestinal barrier are highly complex, and the mechanisms underlying its damage during sepsis require further investigation.

The intestinal mucosal barrier consists of four major components: physical, chemical, immune and microbial. Among these, the physical barrier forms the foundation for maintaining overall function, whilst the mucus layer and intestinal epithelial glycocalyx constitute the core structures of the physical barrier (5).Glycans are widely distributed on the surface of various cell types, with monosaccharides as basic units forming glycoconjugates such as glycosaminoglycans, glycoproteins, proteoglycans and glycolipids (6). Based on distribution, glycans can be classified into endothelial glycans and intestinal epithelial glycans; the latter are crucial for maintaining intestinal barrier stability, regulating substance permeability and defending against bacterial invasion.The intestinal epithelial glycocalyx, together with the mucus layer and epithelial cell layer, forms the frontline of the intestinal defence. During bacterial invasion or stress conditions, the glycocalyx is damaged first, directly leading to increased intestinal permeability. Toxins and inflammatory mediators further penetrate the intestinal wall, activating immune response, and

exacerbating glycocalyx degradation, thereby driving continuous worsening of intestinal injury and systemic inflammation (7,8).The Syndecan family comprises key heparan sulphate proteoglycans that form the glycocalyx scaffold. Among these, Syndecan-1 (CD138) is primarily expressed on epithelial cells and participates in intercellular and cell-matrix adhesion junctions to maintain epithelial morphology and structural stability (9).Its heparan sulfate chains can bind to adhesion molecules, cytokines, chemokines and other factors, regulate inflammatory cell chemotaxis, adhesion and migration, and participate in inflammatory regulation (10). In inflammatory bowel disease (IBD), TNF-α, inducible nitric oxide synthase and other factors can exacerbate glycocalyx disruption, forming a vicious cycle of inflammation and barrier damage (11). However, the interactions between inflammatory mediators and the intestinal epithelial glycocalyx, as well as the upstream and downstream regulatory mechanisms during sepsis, remain incompletely elucidated. A deeper understanding of the molecular mechanisms underlying intestinal epithelial glycocalyx damage in sepsis could provide a theoretical basis for the development of specific intestinal barrier protection strategies.

On the basis of early bundle therapy for clinical sepsis, identifying safe and effective drugs for intestinal barrier protection holds significant value in reducing complications and improving the prognosis of critically ill patients.Somatostatin (SST) is a cyclic peptide widely distributed in the nervous and digestive systems. It exerts effects through SSTR receptors and possesses anti-inflammatory, antioxidant, cytoprotective and immunomodulatory effects (12-15), but whether it can protect the intestinal epithelial glycocalyx and improve intestinal function in sepsis remains unclear.

The pathophysiological process of sepsis is inherently a complex network involving the

coordinated action of multiple genes and proteins; studies focusing on a single molecule struggle to systematically clarify its regulatory mechanisms. The development of high-throughput sequencing technologies has provided new tools for comprehensively elucidating biological processes. Combined transcriptomic and proteomic analyses allows a panoramic understanding of molecular mechanisms at both the transcriptional and protein levels, offering new insights for identifying therapeutic targets (16-17).In this study, by establishing a rat model of sepsis and using multi-omics integrated analysis, we systematically investigated the protective effect of SST against sepsis-induced intestinal epithelial glycocalyx damage, and explored associated molecular profiles and candidate targets via integrated multi-omics analysis, and identified potential therapeutic targets, thereby providing an experimental basis and theoretical support for precise interventions to protect the intestinal barrier in sepsis.

2. Materials and Methods

2.1 Ethical Statement

All animal experimental protocols in this study strictly adhered to the American Veterinary Medical Association (AVMA) Guidelines for the Euthanasia of Laboratory Animals (2020 Edition), the National Institutes of Health (NIH) Guide for the Care and Use of Laboratory Animals (8th Edition), and the Chinese National Standard Guidelines for Ethical Review of Laboratory Animals (GB/T 35892-2018).The experimental protocols were reviewed and approved by the Ethics Committee for Laboratory Animal Welfare at the Affiliated Hospital of Chengde Medical University (Ethics Approval No.: CYFYLL2025638). All experimental procedures strictly followed the 3R principles. By optimising anaesthesia and analgesia protocols and setting humane endpoints, the suffering and stress of the experimental animals were minimized to the

greatest extent possible.

2.2 Establishment of the sepsis animal model

Male specific-pathogen-free(SPF) Sprague-Dawley (SD) rats (8-10 weeks old, weighing 200-250 g) were purchased from Beijing Huafukang Biotechnology Co., Ltd. in Beijing, China (Animal Licence No.: SYXK (Ji) 2021-004).The rats were housed in the SPF standardized laboratory animal facility at the Experimental Centre of the Affiliated Hospital of Chengde Medical University, under conditions of 20-26℃ ambient temperature, 40-70% relative humidity, and a 12-h light-dark cycle. Autoclaved water and SPF-grade rat feed were provided ad libitum. Experiments were performed after 7 days of acclimatization.

A rat model of sepsis was established using the cecal ligation and puncture (CLP) method.Rats were fasted for 12 h before surgery but allowed free access to water. Anaesthesia was induced by intraperitoneal injection of 3% sodium pentobarbital (50 mg/kg). Once the corneal reflex disappeared to confirm adequate anesthesia, rats were fixed, the abdominal skin was shaved and disinfected, and a midline abdominal incision was made to expose the cecum. The distal 1 cm of the caecum was ligated aseptically,punctured twice with a 22G needle, and gently squeezed to release a small amount of intestinal contents. After confirming patency of the puncture site, the abdomen was closed layer by layer. In the sham-operated group, only abdominal opening and cecal exposure were performed without ligation or puncture; the remaining procedures were identical to those in the sepsis group. Animals were observed for 1 h postoperatively before being returned to the animal room.

132 **2.3 Animal Grouping and Treatment**

133 Eighteen rats were randomly divided into three groups: the sham group (sham
134 operation, n = 6), the CLP group (CLP procedure performed, n = 6) and the SST group
135 (CLP + subcutaneous injection of SST, n = 6).

136 Rats in the SST group received subcutaneous injection of 100 μg/kg SST
137 (purchased from MedChemExpress, diluted with saline) immediately after
138 successful modeling; rats in the other two groups received an equal volume of saline
139 subcutaneously.The experiment strictly followed humane end-point criteria: when
140 rats showed severe sepsis symptoms such as lethargy, inability to eat or drink
141 independently, body weight loss >20%, or respiratory distress, they were
142 immediately euthanized by intraperitoneal injection of a lethal dose of sodium
143 pentobarbital (150 mg/kg). All procedures complied with the AVMA guidelines for
144 laboratory animal welfare and euthanasia.24 h after CLP, all rats were euthanized for
145 subsequent experiments.

146 **2.4 Histopathological Examination**

147 Intestinal tissues were fixed in 4% paraformaldehyde, embedded in paraffin
148 using standard techniques, and sectioned into 5-μm-thick slices. Sections were stained
149 with routine hematoxylin and eosin and examined under a BX60-32FB3-E01
150 microscope (Olympus, Tokyo, Japan) at 200× and 400× magnifications.

151 **2.5 Enzyme-Linked Immunosorbent Assay (ELISA)**

152 Venous blood was collected from rats in the three groups at 6, 12 and 24 h after
153 modelling, respectively. Serum supernatants were collected after centrifugation at

3000-4000 rpm for 20 min. The concentration of TNF-α was determined using the Rat TNF-α ELISA Kit (catalogue number GER0004-96T, Servicebio, China).Absorbance at 450 nm were measured using a microplate reader. A standard curve was plotted with standard concentrations on the x-axis and corresponding OD values on the y-axis; TNF-α concentrations in each sample were calculated using the curve equation.

2.6 Western Blotting

Protein extraction was performed using radioimmunoprecipitation assay (RIPA) lysis buffer. After protein concentration determination using the BCA method, 25 μg of protein samples per lane were separated by 6% sodium dodecyl sulfate-polyacrylamide gel electrophoresis (SDS-PAGE). Separated proteins were transferred to a polyvinylidene difluoride (PVDF) membrane and blocked at room temperature with blocking solution containing 5% bovine serum albumin (BSA) to eliminate non-specific binding.Membranes were incubated overnight at 4 ℃ with rabbit anti-TNF-α antibody (1:1000,cat. no. 26405-1-AP, Wuhan Sanying, China), rabbit anti-Syndecan-1 antibody (1:1000, cat. no. 10593-1-AP, Wuhan Sanying, China), and rabbit anti-GAPDH antibody (1:10,000, GB15004, Servicebio, China) .The next day, membranes were incubated with horseradish peroxidase (HRP)-conjugated goat anti-rabbit IgG (1:3000, GB23303, Servicebio, China) at room temperature for 1 h. Protein bands were detected using an enhanced chemiluminescence (ECL) kit.

2.7 Immunofluorescence staining of intestinal tissue

Paraffin-embedded intestinal tissues from the three groups were routinely

dewaxed and subjected to heat-induced antigen retrieval in Tris-EDTA antigen retrieval buffer (pH 8.0) for 30 min using an antigen retriever. After cooling, tissues were blocked with 5% BSA at room temperature for 30 min, then incubated overnight at 4 ℃ with rabbit anti-TNF-α antibody (1:100, cat. no. 26405-1-AP, Servicebio, China) and rabbit anti-Syndecan-1 antibody (1:100, cat. no. GB115052, Servicebio, China). After washing, CY3-labelled goat anti-rabbit IgG secondary antibody (1:300, cat. no. GB21303, ServiceBio, China) was added and incubated in the dark for 1 h, followed by DAPI nuclear staining. Autofluorescence was quenched, and slides were mounted. Images were acquired under a fluorescence microscope at an excitation wavelength of 364 nm and emission wavelength of 454 nm. Fluorescence intensity was analyzed using ServiceBio digital slide browsing software.

2.8 Multi-omics integrated analysis

Total RNA and protein were extracted from intestinal tissues for transcriptomic sequencing and Astral-DIA-based quantitative proteomics analysis. Raw sequencing reads were processed with fastp to remove adapters, trim low-quality 3′/5′ bases (Phred score < 20), discard reads with >10% ambiguous (N) bases, and filter sequences < 20 bp in length. Clean reads were mapped to the reference genome using HISAT2, and gene expression levels were quantified as read counts using RSEM. Differential expression analysis was performed using DESeq2. Screening thresholds for differentially expressed genes (DEGs) were $|\log_2 FC \text{ (fold change)}| \geq 1$ and false discovery rate (FDR) < 0.05. Raw mass spectrometry data were analyzed using Spectronaut™ 19 software against the Rattus norvegicus reference protein

database. The search parameters were as follows: peptide length of 7–52 amino acids; digestion enzyme Trypsin/P with a maximum of 2 missed cleavages; variable modifications including oxidation (M) and acetylation (protein N-terminus); fixed modification of carbamidomethylation (C). Both peptide and protein FDR were controlled at ≤ 0.01, with peptide confidence ≥ 99% and XIC width ≤ 75 ppm. Protein quantification was performed using the MaxLFQ algorithm. Screening criteria for differentially expressed proteins (DEPs) were $p < 0.05$ and fold change (FC) ≥ 1.2. DEGs and DEPs were annotated using the KEGG database. KEGG pathway enrichment analysis was performed using the KOBAS software, with FDR < 0.05 as the threshold for significant enrichment. Protein-protein interaction network analysis was performed using the STRING v11.5 database. Transcriptomic library preparation, high-throughput sequencing, proteomic peptide preparation, mass spectrometry, and subsequent bioinformatics analyses were all performed by Shanghai Biotecan Pharmaceuticals Co., Ltd. (Shanghai, China).

Integrated transcriptomic and proteomic analyses were performed. An integrated dataset was constructed based on the one-to-one correspondence between genes and proteins. Venn diagrams were used to identify common and unique molecules in each omics approach, and Spearman's correlation analysis was used to assess consistency between transcript and protein expression levels. DEGs and DEPs were identified separately, and their expression patterns were visualized using a nine-quadrant plot to analyse overlaps and expression trend similarities/differences. KEGG pathway enrichment analysis was performed on associated molecular sets and

shared DEGs/DEPs to identify enriched pathways and candidate molecules associated with SST-mediated protection against intestinal epithelial glycocalyx injury.

2.9 Validation of candidate targets

2.9.1 Real-time quantitative polymerase chain reaction (RT-qPCR)

Total RNA was extracted from tissues using the TRIzol method (Jiangsu Kaiji Biotechnology Co., Ltd., KGF5101-100, China) and reverse-transcribed into cDNA using the TaKaRa PrimeScript™ RT Kit (TaKaRa, Japan).RT-qPCR was performed under the following conditions: 5-min pre-denaturation at 95℃, 15 s denaturation at 95℃, 1 min annealing at 60℃, for a total of 40 cycles.Primer sequences synthesised by Jiangsu Kaiji Biotechnology Co., Ltd. are as follows:

Aldh1l1-F: 5’ GGCACGGCTCCATCATCTACCA-3’;

Aldh1l1-R: 5’ GCAGCAGAAGGTCACCAGTGTC-3’;

Fgfbp1-F: 5’ GCCTCATCCTGCTCTCTTTCCT-3’;

Fgfbp1-R: 5’ TCCTCCGTTGTGCTGTCTGGTA-3’;

GAPDH-F: 5’ AGGTTGTCTCCTGTGACTTCAA-3’;

GAPDH-R: 5’ CTGTTGCTGTAGCCATATTCATTG-3’.

2.9.2 Western blotting of target proteins

Protein extraction, concentration determination and membrane transfer methods were performed as described in Section 2.6.Membranes were incubated overnight at 4℃ rabbit anti-ALDH1L1 antibody (1:1000, Botron RM9225), rabbit anti-Fgfbp1 (1:1000, abclonal A7458) and rabbit anti-GAPDH antibody (1:5000, Jiangsu Kaiji

Biotechnology Co., Ltd., KGC6102-1,China).The next day, membranes were incubated with HRP-conjugated goat anti-rabbit (1:3000, GB23303, Servicebio, China) for 1 h. Protein bands were detected using an ECL kit.

2.10 Statistical Analysis

All statistical analyses were performed using GraphPad Prism 9.0 (GraphPad Software, San Diego, CA, USA) and SPSS 25.0 (IBM, Chicago, IL, USA). After conducting a normality test, data were analyzed by the Student's t-test or one-way ANOVA followed by Tukey's analysis (for normally distributed data), and showed as the means ± standard deviation (SD). p-value < 0.05 was considered statistically significant. All experiments were carried out at least 3 times independently.

3.Results

3.1 SST ameliorates intestinal injury in septic rats

A rat model of sepsis was successfully established by CLP, and intestinal tissue samples were collected (Figure 1A).HE staining(Figure 1B) showed that intestinal tissue in the sham group had clear structural layers, intact mucosal epithelium, normal epithelial cell morphology, abundant and evenly distributed intestinal villi, densely arranged intestinal glands in the lamina propria, regularly arranged muscle layer cells with normal morphology, and no obvious inflammatory cell infiltration.In the CLP group, epithelial shedding at the villus tips (orange arrows) and exposure of the lamina propria were observed, with inflammatory cell infiltration in the lamina propria (blue arrows). After SST treatment, mild separation between epithelial cells and the lamina propria was seen at the tips of some intestinal villi (green arrows), and inflammatory cell infiltration was milder than in the CLP group.

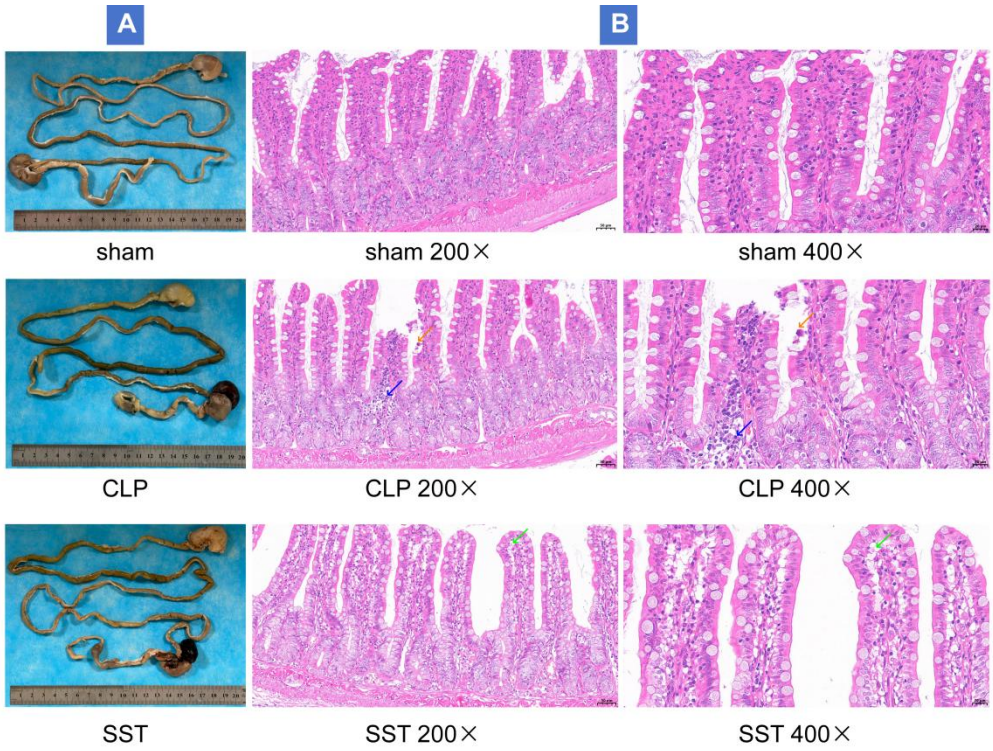


Figure 1: SST alleviates intestinal damage in rats with sepsis. (A) Intestinal tissues from sham, CLP and SST groups. (B) Histopathological features assessed by HE staining. Magnification: 200× and 400×; scale bar: 50 μm. n = 6 per group.

3.2 SST suppresses inflammation and protects the intestinal epithelial glycocalyx

ELISA results showed that compared with the 6-h time point, serum TNF-α concentrations in the CLP group were elevated at 12 and 24 h. In the SST group, TNF-α was increased at 12 h but showed a downward trend at 24 h ($P < 0.05$).Compared with the sham group, serum TNF-α was significantly elevated in the CLP group ($P < 0.05$), while TNF-α in the SST group was lower than in the sepsis group (Figure 2A).

Western blot analysis of intestinal tissue showed that TNF-α expression was increased and Syndecan-1 expression was decreased in the CLP group. After SST treatment, TNF-α expression was reduced and Syndecan-1 expression was restored (Figure 2B).

Immunofluorescence staining showed that TNF-α (red fluorescence) was weakly and

diffusely expressed in the intestinal mucosa of the Sham group (Figure 2C a, d, g).Compared with the sham group, TNF-α fluorescence intensity was significantly enhanced in the CLP group, with positive signals widely distributed in the intestinal mucosal layer and around the glands, indicating severe local intestinal inflammation (Figure 2C b, e, h).After SST intervention, TNF-α fluorescence intensity was markedly decreased, and the positive expression range in inflammatory areas was reduced (Figure 2C c, f, i).

For Syndecan-1, continuous and uniform linear distribution along the apical surface of intestinal epithelial cells was observed in the sham group(red fluorescence signal),closely matching the epithelial outline labeled by DAPI (blue fluorescence), indicating an intact glycocalyx structure and stable Syndecan-1 expression (Figure 2D a, d, g). In the CLP group, the membrane distribution of Syndecan-1 was disrupted and fluorescence intensity was significantly reduced (Figure 2D b, e, h).After SST treatment, Syndecan-1 fluorescence intensity was recovered, and the linear distribution pattern on the epithelial surface was partially restored (Figure 2D c, f, i).

Semi-quantitative analysis confirmed that compared with the sham group, the mean fluorescence intensity of TNF-α was significantly increased and that of Syndecan-1 was significantly decreased in the CLP group ($P < 0.0001$). In the SST group, TNF-α expression was lower than in the CLP group ($P < 0.05$), and Syndecan-1 expression was higher ($P < 0.01$). These results indicate that SST effectively inhibits sepsis-induced intestinal inflammation, alleviates intestinal epithelial glycocalyx damage, and reduces Syndecan-1 shedding.

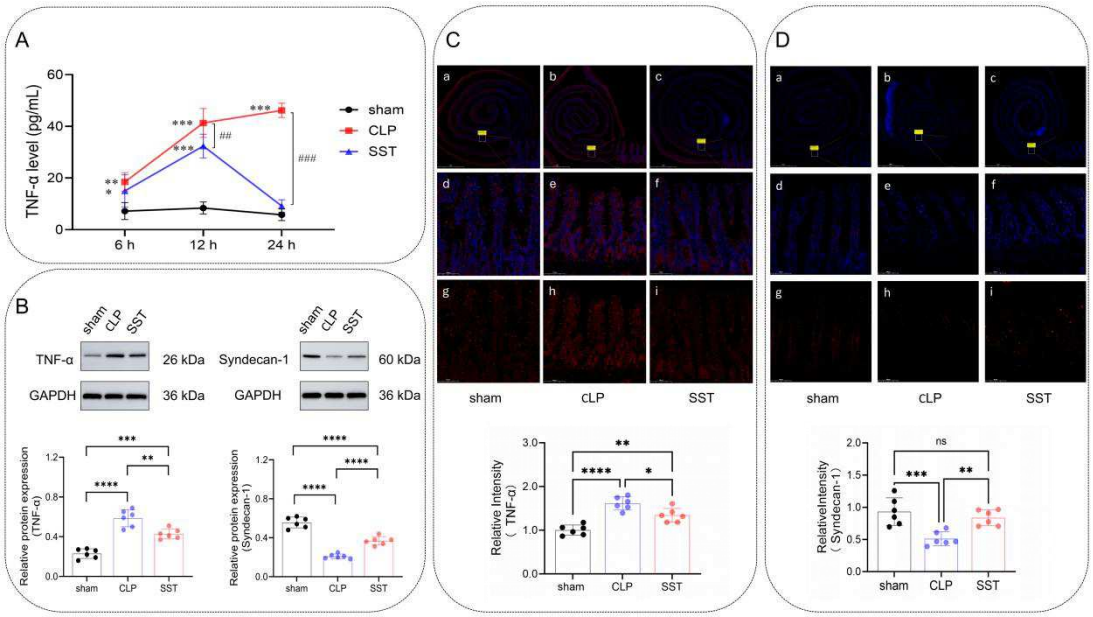


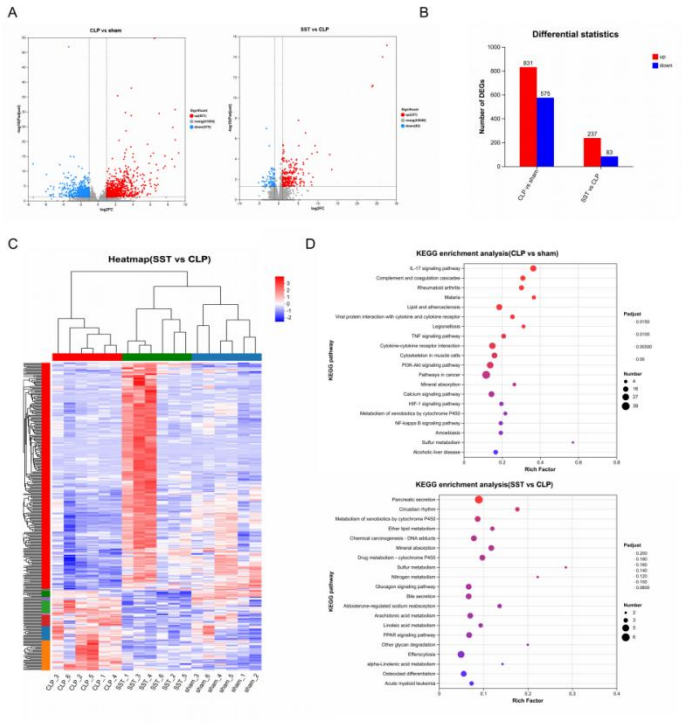
Figure 2: SST inhibits inflammation and protects the intestinal epithelial glycocalyx in septic rats. (A) Serum TNF-α levels detected by ELISA at different time points. $^{*}P < 0.05$, $^{**}P < 0.01$, $^{***}P < 0.001$ vs. sham; $^{\#\#}P < 0.01$, $^{\#\#\#}P < 0.001$ vs. CLP. (B) Western blot analysis of TNF-α and Syndecan-1 in intestinal tissue. $^{*}P < 0.05$, $^{**}P < 0.01$, $^{***}P < 0.001$, $^{****}P < 0.0001$. (C) Immunofluorescence analysis of TNF-α in intestinal tissue. (a-c) Low-magnification overview, scale bar: 2 mm; (d-f) high-magnification details, scale bar: 100 μm; (g-i) Single-channel validation, scale bar: 100 μm. $^{*}P < 0.05$, $^{**}P < 0.01$, $^{***}P < 0.001$, $^{****}P < 0.0001$. (D) Immunofluorescence analysis of Syndecan-1 in the small intestine.(a-c) Low-magnification overview, scale bar: 2 mm; (d-f) high-magnification details, scale bar: 100 μm; (g-i) Single-channel validation, scale bar: 100 μm. $^{*}P < 0.05$, $^{**}P < 0.01$, $^{***}P < 0.001$, $^{****}P < 0.0001$. Data are presented as the mean ± standard deviation. n = 6 per group.

3.3 Transcriptomic and proteomic profiling

Transcriptomic analysis showed that compared with the sham group, 831 genes were significantly up-regulated and 575 genes were down-regulated in the CLP group. Compared with

the CLP group, 237 genes were up-regulated and 83 genes were down-regulated in the SST group. Heatmap analysis showed moderate reproducibility within groups and significant differences between groups.KEGG enrichment analysis showed that DEGs between sham and CLP groups were mainly enriched in the IL-17 signaling pathway, complement and coagulation cascades, and NF-κB pathway, while DEGs between SST and CLP groups were mainly enriched in pancreatic secretion, circadian rhythm, and PPAR signaling pathway (Figure 3).

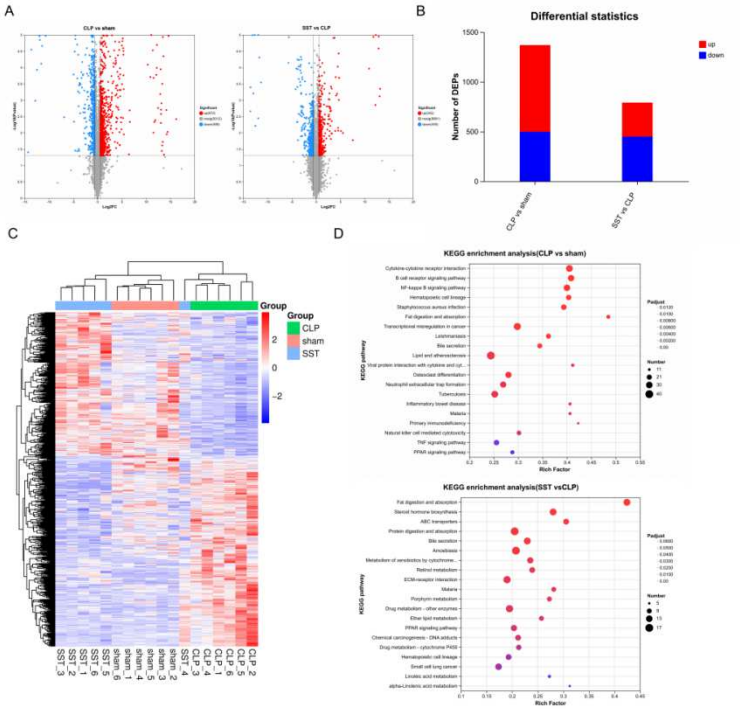
Proteomic analysis showed that compared with the sham group, 872 proteins were up-regulated and 498 proteins were down-regulated in the CLP group. Compared with the CLP group, 342 proteins were significantly up-regulated and 449 proteins were down-regulated in the SST group. KEGG enrichment analysis showed that DEPs between sham and CLP groups were mainly enriched in cytokine-cytokine receptor interaction, NF-κB signaling pathway, transcriptional misregulation in cancer, and PPAR signaling pathway; DEPs between SST and CLP groups were mainly enriched in fat digestion and absorption, steroid hormone biosynthesis, protein digestion and absorption, and PPAR signaling pathway (Figure 4).



327

328 **Figure 3** Transcriptomic analysis results. (A) Volcano plot. (B) Statistics of DEGs between groups.

329 (C) Clustering heatmap. (D) KEGG enrichment analysis.



330

331 **Figure 4** Proteomic analysis results. (A) Volcano plot. (B) Statistics of DEPs between groups. (C)

Clustering heatmap. (D) KEGG enrichment analysis.

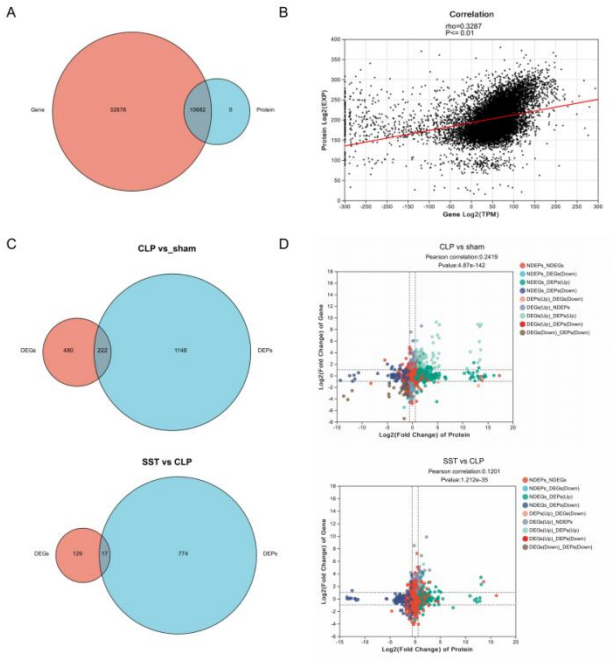
3.4 Multi-omics integrated analysis

To systematically elucidate the molecular regulatory features under the CLP model and SST intervention, an integrated analysis of transcriptomic and proteomic data was first conducted. Venn diagram (Figure 5A) showed that a total of 32,678 genes and 1,082 proteins were identified, of which 1,082 molecules were detected in both omics datasets.Correlation analysis (Figure 5B) showed a moderately significant positive correlation between gene and protein expression levels (rho = 0.3287, $P < 0.01$), indicating overall consistency in transcriptional and translational regulation, while also reflecting the important influence of post-transcriptional regulation on protein expression.

After CLP modelling, 480 DEGs and 1,148 DEPs were identified between CLP and Sham groups, of which 222 molecules were differentially expressed at both levels, indicating extensive transcriptional and translational reprogramming induced by CLP. Following SST intervention, 129 DEGs and 774 DEPs were identified between SST and CLP groups, with only 17 molecules showing co-differential expression at both transcriptomic and proteomic levels (Figure 5C). Further analysis revealed a significant positive correlation between DEGs and DEPs in the CLP vs. sham comparison (Pearson r = 0.2419, $P < 0.001$), with a large number of molecules exhibiting consistent up- or down-regulation trends at both the gene and protein levels. However, the correlation was significantly reduced in the SST vs. CLP comparison (Pearson r = 0.1201, $P < 0.001$), suggesting that SST may exert protective effects mainly through post-translational regulation (Figure 5D). Furthermore, proteins abnormally expressed in the CLP group showed an opposite expression trend after SST intervention, indicating that SST can effectively reverse

CLP-induced protein dysregulation (Figure 5D).

KEGG enrichment analysis further revealed that after CLP modelling, both gene and protein levels were significantly enriched in inflammation-related pathways, indicating that excessive inflammatory response is a core pathological feature of CLP-induced intestinal injury. After SST intervention, pathways related to lipid metabolism and mitochondrial function were significantly enriched. Among them, the PPAR signaling pathway was significantly enriched in both transcriptome and proteome, which plays a candidate role in regulating metabolic homeostasis, inhibiting inflammation, and maintaining mitochondrial function, suggesting that it may mediate the protective effects of SST (Figure 5E).



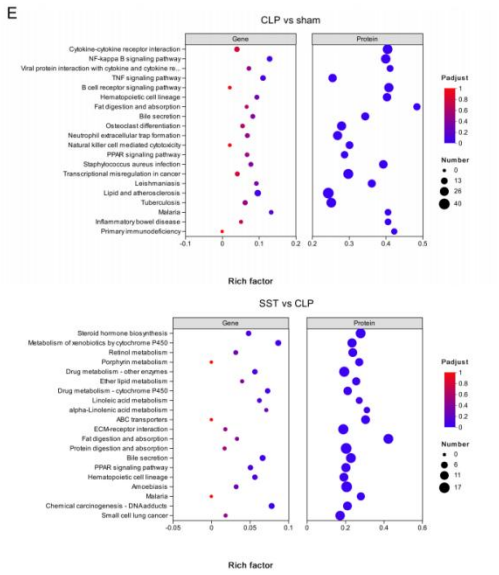


Figure 5 Multi-omics integrated analysis results. (A) Venn diagram of transcriptomics and proteomics. (B) Correlation scatter plot. (C) Venn diagram of DEGs/DEPs. (D) Nine-quadrant plot. (E) KEGG enriched pathway diagram.

3.5 Validation of FGFBP1 and ALDH1L1 as candidate targets

Venn diagrams based on joint analysis of DEGs/DEPs (Figure 6A, B) showed no overlapping targets between up-regulated genes/proteins in the CLP group and down-regulated genes/proteins in the SST group, while the intersection of down-regulated genes/proteins in the CLP group and up-regulated genes/proteins in the SST group identified **FGFBP1** and **ALDH1L1**. Box plots (Fig. 6C, D) indicated that these two molecules may be candidate targets for SST in ameliorating sepsis-associated intestinal injury.

RT-PCR results (Figure 6E) showed that mRNA expression levels of *Fgfbp1* and *Aldh1l1* in intestinal tissue were significantly lower in the CLP group than in the sham group. After SST intervention, their mRNA levels were significantly higher than in the CLP group ($P <$

0.01).Western blot analysis (Figure 6F) confirmed that protein expression levels of FGFBP1 and ALDH1L1 were significantly decreased in the CLP group and significantly restored after SST treatment ($P < 0.01$).These results validate FGFBP1 and ALDH1L1 as candidate targets of SST against sepsis-induced intestinal epithelial glycocalyx damage.

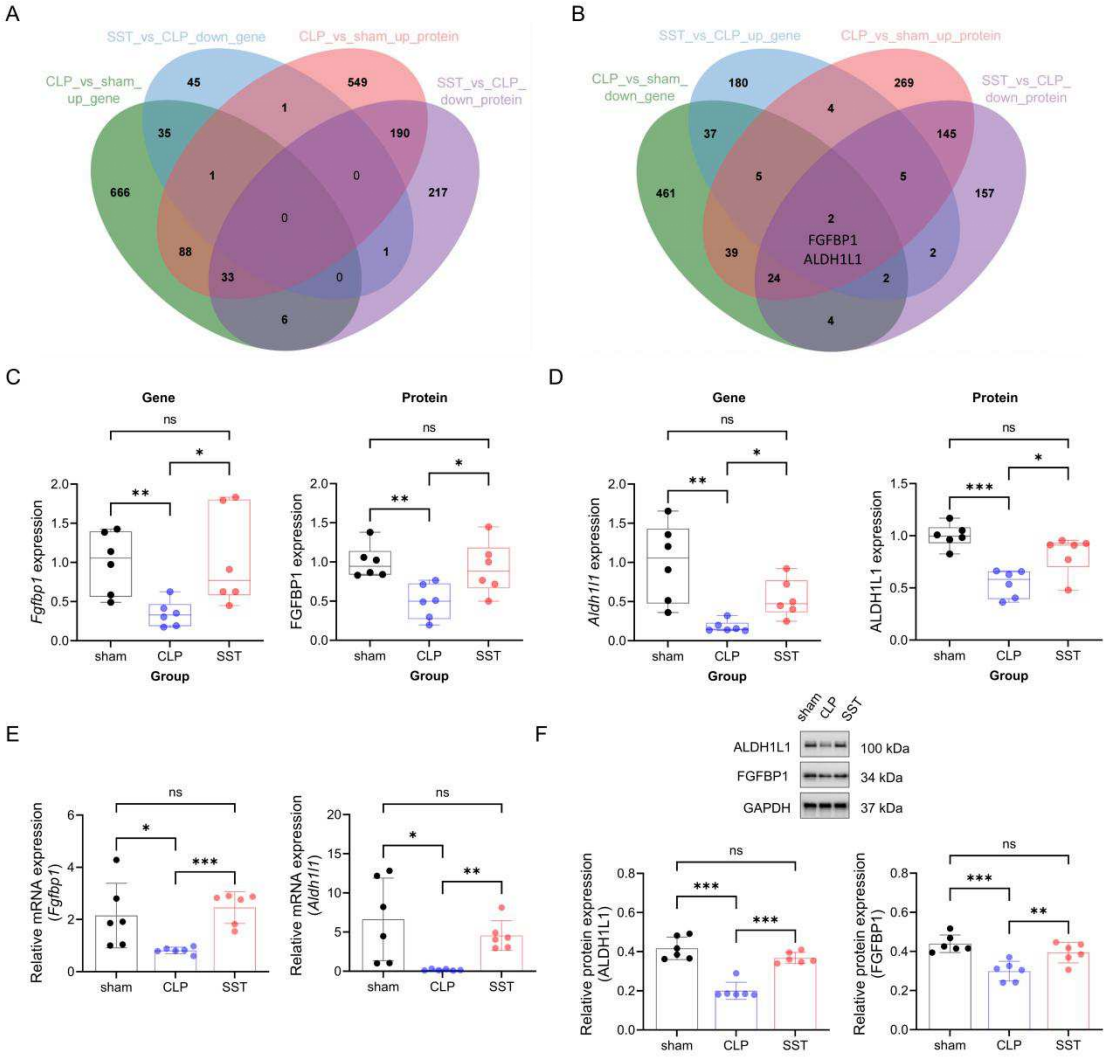


Figure 6 Validation of FGFBP1 and ALDH1L1 as key targets. (A, B) Venn diagrams of DEGs/DEPs. (C, D) Box plots of *Fgfbp1* / FGFBP1 and *Aldh1l1* / ALDH1L1 expression. (E) mRNA levels detected by RT-qPCR. (F) Protein levels detected by Western blot. $^{*}P < 0.05$, $^{**}P < 0.01$, $^{***}P < 0.001$.

4.Discussion

In this study, a rat model of sepsis was successfully established using the CLP method. ELISA results showed that serum TNF-α levels in the sepsis group increased progressively over time and were significantly higher than in the sham group at the same time point, confirming that this model reliably reproduces the typical pathophysiological process of sepsis.

HE staining showed structural damage to intestinal tissue in CLP rats, Western blot and immunofluorescence results showed significantly elevated TNF-α levels compared with the control group, confirming the destructive effect of TNF-α-dominated inflammatory storm on intestinal mucosa and epithelial structure during sepsis. The glycocalyx is a crucial physical barrier covering the surface of intestinal epithelial cells and a primary target of early damage in sepsis, and its destruction degree is closely related to sepsis progression (18). Our results showed that the intestinal epithelial glycocalyx was severely impaired in septic rats,with the core marker Syndecan-1 cleaved and shed from the epithelial surface, leading to decreased fluorescence intensity and protein expression. These findings are consistent with previous studies (19), indicating that inflammation-related glycocalyx damage is a key factor leading to intestinal mucosal barrier dysfunction and directly participates in the occurrence and development of intestinal dysfunction in sepsis.

Previous studies have confirmed that SST protects the intestinal mucosal barrier, which may be related to its inhibition of pro-inflammatory factors such as TNF-α released by macrophages, T cells and other immune cells, thereby alleviating excessive inflammatory responses (20,21). In this study, unlike the persistent elevation of serum TNF-α in the CLP group, TNF-α in the SST treatment group peaked at 12 h and then decreased, remaining lower than in the CLP group at 6,

12 and 24 h, indicating that SST effectively inhibits the systemic inflammatory response in septic rats. Meanwhile, HE staining showed that SST alleviated intestinal pathological damage, reduced inflammatory cell infiltration, and improved the structural integrity of the intestinal epithelium. Western blot and immunofluorescence results showed that SST intervention restored Syndecan-1 expression and inhibited TNF-α expression in intestinal tissue of septic rats, confirming that SST can protect the intestinal epithelial glycocalyx structure by suppressing pro-inflammatory factor release.

Transcriptomic and proteomic enrichment analyses further revealed that DEGs and DEPs between groups were enriched in NF-κB and PPAR signaling pathways, suggesting that SST exerts anti-inflammatory and intestinal protective effects at least partially by regulating these pathways. The NF-κB signaling pathway is a typical inflammatory cascade that can enzymatically degrade the glycocalyx structure, aggravate oxidative stress damage, and ultimately lead to glycocalyx shedding, flora imbalance and inflammatory amplification (22,23). Studies have shown that SST inhibits the elevation of pro-inflammatory factors in sepsis animal models by mediating NF-κB pathway regulation, thereby increasing the levels of anti-inflammatory factors (24). Combined with previous studies and our results, the TNF-α-centered inflammatory storm and Syndecan-1 shedding constitute the typical phenotype of intestinal barrier damage in sepsis, while SST can reverse these changes and protect the intestinal epithelial glycocalyx.

Integrated multi-omics analysis showed that sepsis-induced intestinal injury is characterized by simultaneous up-regulation of inflammatory responses at both transcriptional and translational levels. However, SST does not merely inhibit inflammatory gene transcription, but

reverses abnormal protein expression and regulates lipid metabolism and mitochondrial function to exert protective effects. The PPAR signaling pathway was significantly enriched in both omics datasets, suggesting it as a candidate pathway potentially involved in SST-mediated intestinal protection. Regarding the intestinal epithelial mucus layer, PPARγ can up-regulate the expression of MUC1 and other MUC family members (25), which are essential components of the mucus layer (26,27). In addition, PPARγ induces antioxidant enzymes such as SOD2 to neutralize reactive oxygen species (ROS) (28), thereby reducing oxidative stress and promoting mucus layer repair and reinforcement (29). PPARγ antagonizes the transcriptional activity of NF-κB by directly binding to p65 protein, competitively sequestering CBP/p300 co-factors, stabilizing IκBα, and inhibiting IKK kinase (30-33), thereby inhibiting pro-inflammatory factor release. Conversely, NF-κB also inhibits PPARγ expression (34), forming a negative feedback loop.

Furthermore, combined omics Venn diagram showed that the intersection of down-regulated genes/proteins in the CLP group and up-regulated genes/proteins after SST treatment included FGFBP1 and ALDH1L1. ALDH1L1 is a key NADPH-producing enzyme in the liver. Serine is catabolized through the SHMT1-MTHFD1-ALDH1L1 enzymatic cascade to specifically produce NADPH (35), enhance antioxidant capacity, and act as a key ROS scavenger in the antioxidant system (36,37). ROS can promote inflammation by activating upstream signaling molecules such as IKK and MAPK, thereby initiating NF-κB nuclear translocation and enhancing its transcriptional activity (38,39), damaging the endothelial glycocalyx and tight junctions (40). In summary, ALDH1L1 promotes NADPH production, enhances antioxidant capacity, and may alleviate inflammatory responses by inhibiting ROS-mediated NF-κB activation, thereby helping to suppress intestinal epithelial glycocalyx shedding.

FGFBP1 enhances the activity of fibroblast growth factors (FGF1, FGF2) and promotes FGF signaling (41), thereby amplifying pro-inflammatory and pro-fibrotic effects (42-44).However, FGFBP1 plays a positive role in intestinal regeneration and liver injury protection (45,46), and FGF1 expression is negatively correlated with IBD severity.In DSS-induced and TNBS-induced colitis mouse models, FGF1 expression decrease with disease progression (47). This controversy highlights the necessity and importance of in-depth research on FGFBP1, and increases the exploratory value of this study.

This study has several limitations. First, this study is primarily a phenotypic intervention and target screening study. Although ALDH1L1 and FGFBP1 were identified through multi-omics screening and validated by RT-qPCR and Western blot, functional experiments (e.g., knockdown, overexpression, or pharmacological agonism/antagonism) were not performed. Therefore, causal relationships cannot be established, and these molecules should be considered candidate targets rather than confirmed mediators. Future studies employing siRNA knockdown or CRISPR-based editing in intestinal epithelial cell lines are warranted to establish causality. Second, intestinal barrier function was not directly assessed by permeability assays (e.g., FITC-dextran, TEER, or in vivo leakage tests). Consequently, claims regarding "barrier protection" are based on histological and single-marker (Syndecan-1) observations rather than functional integrity measurements.Direct barrier function assessments will be essential in follow-up studies to confirm the functional relevance of these histological findings. Third, glycocalyx integrity was evaluated solely by Syndecan-1, which represents only one component of the glycocalyx scaffold. Other constituents (e.g., mucins, heparan sulfate chains, other proteoglycans) were not examined, limiting the comprehensiveness of our glycocalyx assessment. Fourth, the integrated transcriptomic and

proteomic analysis revealed limited overlap (only 17 co-differentially expressed molecules between SST and CLP groups), suggesting substantial post-transcriptional regulation. The biological significance of this discordance warrants further investigation. Finally, SST was administered immediately after CLP, which is more prophylactic than therapeutic. This limits direct clinical translation, as human sepsis is typically treated after diagnosis rather than at the onset of insult. Delayed intervention protocols mimicking clinical practice are needed to enhance translational relevance. Despite these limitations, our findings provide reliable experimental evidence and new insights for the clinical application of SST in sepsis.

Conclusions

Our study confirms that SST can maintain intestinal epithelial glycocalyx integrity, alleviate intestinal pathological damage, and suppress systemic inflammatory responses during sepsis. Multi-omics analysis indicates that CLP-induced intestinal epithelial glycocalyx damage is characterized by concurrent up-regulation of inflammatory responses at both transcriptional and translational levels. The PPAR signaling pathway is significantly enriched in both transcriptomics and proteomics analyses, suggesting that it may be a candidate pathway mediating the protective effect of SST on the intestinal epithelium during sepsis. ALDH1L1 and FGFBP1 are verified as candidate molecules associated with the protective effect of SST against sepsis-induced intestinal epithelial glycocalyx damage.

Declarations

1. Abbreviations

CLP:Cecal ligation and puncture; SST:Somatostatin; TNF-α:Tumor necrosis factor-α; HE:Hematoxylin-Eosin Staining; ELISA:Enzyme-Linked Immunosorbent Assay; WB:Western

blot; IF:immunofluorescence; RT-qPCR:Reverse transcription-quantitative polymerase chain reaction; NF-κB:Nuclear factor-kappa B; PPAR:Peroxisome proliferator-activated receptor; FGFBP1:Fibroblast growth factor binding protein 1; ALDH1L1:Aldehyde dehydrogenase 1 family member L 1; GAPDH:Glyceraldehyde-3-phosphate dehydrogenase; DEGs:Differentially expressed genes; DEPs:Differentially expressed proteins; KEGG:Kyoto Encyclopedia of Genes and Genomes.

2. Ethics approval and consent to participate

The animal experimental protocol was approved by the Animal Ethics Committee of the Affiliated Hospital of Chengde Medical University (Ethics Approval No.: CYFYLL2025638).

3. Consent for publication

This manuscript has not been published or presented elsewhere in part or in entirety and is not under consideration by another journal. All the authors have approved the manuscript and agree to submission to your esteemed journal.

4. Availability of data and materials

The datasets used in the current study are available from the corresponding author upon reasonable request.

5. Competing interests

The authors declare that they have no competing interests.

6. Funding

This study was supported by 2026 Hebei Provincial Government-funded Training Program for Excellent Talents in Clinical Medicine (No.ZF2026388) and 2024 Hebei Provincial Government-funded Training Program for Excellent Talents in Clinical Medicine

(No.ZF2024008).

7. Authors' contributions

Conceptualization: J.D.X. and Q.S.D.; Methodology: J.D.X., Z.L.M.; Formal analysis: J.D.X., J.X.P.; Investigation: J.D.X., Z.L.M., J.X.P., K.Z., X.R.Y.; Resources: Q.S.D.; Writing - original draft: J.D.X.; Writing - review & editing: Q.S.D.; Supervision: Q.S.D.; Funding acquisition: Q.S.D. All authors have read and approved the final manuscript.

8. Data availability statement

The datasets presented in this study can be found in online repositories. The names of the repository/repositories and accessionnumber(s) can be found below: https://www.ncbi.nlm.nih.gov/, PRJNA1153631.

9. Acknowledgements

Not applicable.

10. Clinical trial number

not applicable.

References

1. Singer M, Deutschman CS, Seymour CW, et al. The Third International Consensus Definitions for Sepsis and Septic Shock (Sepsis-3)[J]. *JAMA*. (2016) 315(8):801-10.doi: 10.1001/jama.2016.0287.

2. Holub M, Závada J. Clinical aspects of sepsis[J]. *Contrib Microbiol.* (2011) 17:12-30.doi:10.1159/000323983.

3. Dong L, Li H, Zhang S, et al.Identification of genes related to consecutive trauma-induced sepsis via gene expression profiling analysis[J]. *Medicine*. (2018) 97(15):e0362.doi:

10.1097/MD.0000000000010362.

4. Haussner F, Chakraborty S, Halbgebauer R, et al. Challenge to the Intestinal Mucosa During Sepsis[J]. *Front Immunol*. (2019) 10:891. doi:10.3389/fimmu.2019.00891.

5. Schneider H, Pelaseyed T, Svensson F, et al. Study of mucin turnover in the small intestine by in vivo labeling[J]. *Sci Rep*. (2018) 8(1):5760. doi:10.1038/s41598-018-24148-x.

6. Wigén J, Elowsson-Rendin L, Karlsson L, et al. Glycosaminoglycans: A Link Between Development and Regeneration in the Lung[J].*Stem Cells Dev*. (2019) 28(13):823-832.doi:10.1089/scd.2019.0009.

7. Segrist E, Cherry S.Using Diverse Model Systems to Define Intestinal Epithelial Defenses to Enteric Viral Infections[J]. *Cell Host Microbe*. (2020) 27(3):329-344. doi:10.1016/j.chom.2020.02.003.

8. An J，Liu YQ，Wang YQ，et al. The Role of Intestinal Mucosal Barrier in Autoimmune Disease: A Potential Target[J]. *Front Immunol*. (2022) 13: 871713.doi：10.3389/fimmu.2022.871713.

9. Becker BF, Jacob M, Leipert S, et al.Degradation of the endothelial glycocalyx in clinical settings: Searching for the sheddases[J].*Br J Clin Pharmacol*. (2015) 80(3):389-402.doi: 10.1111/bcp.12629.

10. Teng YH, Aquino RS,Park PW.Molecular functions of syndecan-1 in disease[J]. *Matrix Biol.* (2012) 31(1):3-16.doi: 10.1016/j.matbio.2011.10.001.

11. Hu C, Liao S, Lv L, et al.Intestinal Immune Imbalance is an Alarm in the Development of IBD[J]. *Mediators Inflamm.* (2023) 2023: 1073984.doi: 10.1155/2023/1073984.

12. Li J, You C, Li Y, et al.Structural basis for activation of somatostatin receptor 5 by cyclic neuropeptide agonists[J].*Proceedings of the National Academy of Sciences*. (2025)

121(6):e2321710121.doi:10.1073/pnas.2321710121.

13. Julian MW, Bao SY, Knoell DL, et al. Intestinal epithelium is more susceptible to cytopathic injury and altered permeability than the lung epithelium in the context of acute sepsis[J].*Int J Exp Pathol*. (2011) 92(5):366-76.doi: 10.1111/j.1365-2613.2011.00783.x.

14. Kim D, Nam HJ, Lee W, et al.PKCα-LSD1-NF-κB-Signaling Cascade Is Crucial for Epigenetic Control of the Inflammatory Response[J]. *Molecular cell*. (2018) 69(3):398-411.e6.doi: 10.1016/j.molcel.2018.01.002.

15. Antonangeli F,Natalini A, Garassino MC, et al. Regulation of PD-L1 Expression by NF-κB in Cancer[J]. *Front Immunol*. (2020) 25:11:584626.doi: 10.3389/fimmu.2020.584626.

16. Chen H, Xue H, Tang X, et al. Identification of a novel sepsis prognosis model: Based on transcriptome and proteome analysis[J].*Shock*. (2024) 62(2):217-226.doi: 10.1097/SHK.0000000000002388.

17. Figueirêdo Leite GG, Ferreira BL, Tashima AK, et al.Combined Transcriptome and Proteome Leukocyte's Profiling Reveals Up-Regulated Module of Genes/Proteins Related to Low Density Neutrophils and Impaired Transcription and Translation Processes in Clinical Sepsis[J].*Front Immunol*. (2021) 12:744799.doi: 10.3389/fimmu.2021.744799. eCollection 2021.

18. Chen S, He Y, Hu Z, et al. Heparanase Mediates Intestinal Inflammation and Injury in a Mouse Model of Sepsis[J].*J Histochem Cytochem*. (2017) 65(4):241-249.doi:10.1369/0022155417692536.

19. van Golen RF, van Gulik TM, Heger M. Mechanistic overview of reactive species-induced degradation of the endothelial glycocalyx during hepatic ischemia/reperfusion injury[J]. *Free Radic Biol Med*. (2012) 52(8): 1382-1402.doi: 10.1016/j.freeradbiomed.2012.01.013.

585 20. Algaba-Chueca F, de-Madaria E, Lozano-Ruiz B, et al.The expression and activation of the
586 AIM2 inflammasome correlates with inflammation and disease severity in patients with acute
587 pancreatitis[J]. *Pancreatology*. (2017) 17(3):364-371.doi: 10.1016/j.pan.2017.03.006.
588 21. Lamrani A, Tulliez M, Chauvelot-Moachon L, et al. Effects of octreotide treatment on early
589 TNF-alpha production and localization in experimental chronic colitis[J]. *Aliment Pharmacol Ther*.
590 (1999) 13(5):583-94.doi:10.1046/j.1365-2036.1999.00515.x.
591 22. Day RM, Mitchell TJ, Knight SC, et al.Regulation of epithelial syndecan-1 expression by
592 inflammatory cytokines[J]. *Cytokine*. (2003) 21(5):224-233.doi:10.1016/s1043-4666(03)00091-7.
593 23. Zhang Y, Wang Z, Liu J, et al. Cell surface-anchored syndecan-1 ameliorates intestinal
594 inflammation and neutrophil transmigration in ulcerative colitis[J]. *J Cell Mol Med*. (2017)
595 21(1):13-25. doi:10.1111/jcmm.12934.
596 24. Xu, X;Zhu Q;Li G,et al.Protective Role of Somatostatin in Sepsis-Induced Intestinal Barrier
597 Dysfunction through Inhibiting the Activation of NF-κB Pathway[J].*Gastroenterology Research &*
598 *Practice*. (2020) 2020:1-8.doi:10.1155/2020/2549486.
599 25. Yong SP, Erik PL, Kosuke K, et al.PPARγ inhibits airway epithelial cell inflammatory
600 response through a MUC1-dependent mechanism[J].*Am J Physiol Lung Cell Mol Physiol*. (2012)
601 302(7):L679-87.doi:10.1152/ajplung.00360.2011. Epub 2012 Jan 20.
602 26. Jia L, Alan JS, Caroline VH,et al.Identification and multimodal characterization of a
603 specialized epithelial cell type associated with Crohn's disease[J]. *Nat Commun*. (2024)
604 15(1):7204.doi: 10.1038/s41467-024-51580-7.
605 27. Vasso A, Lily S, Sharron EG.MUC1 (CD227): a multi-tasked molecule[J].*Cell Mol Life Sci*.
606 (2015) 72(23):4475-500.doi:10.1007/s00018-015-2014-z.

28. Yonggang Y, Xiaolong F, Ling T, et al. Dendrobine alleviates CCl4-induced acute liver injury by inhibiting necroptosis through activation of the Nrf2/PPARγ/SOD2 signaling pathways[J].*Chin Med*. (2025) 20(1):182. doi:10.1186/s13020-025-01241-8.

29. Sarah A, Mardeen K, Mark L,et al.Hemorrhagic Shock and Resuscitation Causes Glycocalyx Shedding and Endothelial Oxidative Stress Preferentially in the Lung and Intestinal Vasculature[J]. *Shock*. (2021) 56(5):803-812.doi: 10.1097/SHK.0000000000001764.

30. Fei C, Muchun W, J PO,et al.Phosphorylation of PPARgamma via active ERK1/2 leads to its physical association with p65 and inhibition of NF-kappabeta[J]. *J Cell Biochem*. (2003) 90(4):732-44.doi: 10.1002/jcb.10668.

31. Ying K, Yan G, Dongyi L,et al.Trans-repression of NFκB pathway mediated by PPARγ improves vascular endothelium insulin resistance[J]. *J Cell Mol Med*. (2019) 23(1):216-226. doi: 10.1111/jcmm.13913.

32. Fan Y, Wenjing Y, Mingyuan C, et al.PPARγ agonist alleviates sepsis-related liver injury by modulating M1/M2 macrophage polarization via the PPARγ/IκBα/NF-κB pathway[J]. *Life Sci*. (2025) 379:123881. doi:10.1016/j.lfs.2025.123881.

33. Gregory SH, Michael TL, Christopher KG. PPARs and lipid ligands in inflammation and metabolism[J]. *Chem Rev*. (2011) 111(10):6321-40.doi:10.1021/cr2001355.

34. Eleni M, Maud B, Natalie C,et al.Crosstalk between the canonical NF-κB and Notch signaling pathways inhibits Pparγ expression and promotes pancreatic cancer progression in mice[J]. *J Clin Invest*. (2011) 121(12):4685-99.doi: 10.1172/JCI45797.

35. Zhaoyue Z, Tara T, Xincheng X, et al.Serine catabolism generates liver NADPH and supports hepatic lipogenesis[J]. *Nat Metab*. (2021) 3(12):1608-1620.doi: 10.1038/s42255-021-00487-4.

36. Leah EJ, Patrick CB. Effects of aging and anti-aging dietary restriction on regulators of the [NADPH]/[NADP+] in different neural cell types and brain regions[J]. *Free Radic Biol Med*. (2025) 240:745-772.doi: 10.1016/j.freeradbiomed.2025.09.001.

37. Yi-Lin Z, Ying A, Li-Juan S, et al. NADPH-dependent ROS accumulation contributes to the impaired osteogenic differentiation of periodontal ligament stem cells under high glucose conditions[J]. *Front Endocrinol (Lausanne)*. (2023) 14:1152845. doi:10.3389/fendo.2023.1152845.

38. Juanli F, Qiong S, Xiufang S, et al.Tetrachlorobenzoquinone exhibits neurotoxicity by inducing inflammatory responses through ROS-mediated IKK/IκB/NF-κB signaling[J]. *Environ Toxicol Pharmacol*. (2016) 41:241-50. doi: 10.1016/j.etap.2015.12.012.

39. Jungwon K, Nara T, Byung SM, et al.Malabaricone C suppresses lipopolysaccharide-induced inflammatory responses via inhibiting ROS-mediated Akt/IKK/NF-κB signaling in murine macrophages[J]. *Int Immunopharmacol*. (2012) 14(3):302-10.doi: 10.1016/j.intimp.2012.08.006.

40. Gianfranco UM, Anna-Maria GP.The Glucocorticoid System: A Multifaceted Regulator of Mitochondrial Function, Endothelial Homeostasis, and Intestinal Barrier Integrity[J]. *Semin Respir Crit Care Med*. (2026) 47(1):32-46. doi:10.1055/a-2684-3689.

41. Tassi E, Al-Attar A, Aigner A, et al. Enhancement of fibroblast growth factor (FGF) activity by an FGF-binding protein[J]. *J Biol Chem*. (2001) 276(43):40247-53. doi:10.1074/jbc.M104933200.

42. Masaru Y, Tetuo M, Tomoko T, et al. Submucosal fibrosis and basic-fibroblast growth factor-positive neutrophils correlate with colonic stenosis in cases of ulcerative colitis[J]. *Digestion*. (2011) 84(1):12-21. doi:10.1159/000320773.

651 43. Strutz F, Zeisberg M, Renziehausen A, et al. TGF-beta 1 induces proliferation in human renal
652 fibroblasts via induction of basic fibroblast growth factor (FGF-2)[J]. *Kidney Int*. (2001)
653 59(2):579-92. doi:10.1046/j.1523-1755.2001.059002579.x.
654 44. Chundong Y, Fen W, Chengliu J, et al. Role of fibroblast growth factor type 1 and 2 in carbon
655 tetrachloride-induced hepatic injury and fibrogenesis[J]. *Am J Pathol*. (2003)
656 163(4):1653-62. doi:10.1016/S0002-9440(10)63522-5.
657 45. Claudia C, Jonathan M, Liang C, et al. Time-resolved fate mapping identifies the intestinal
658 upper crypt zone as an origin of Lgr5+ crypt base columnar cells[J]. *Cell*. (2024)
659 187(12):3039-3055.e14. doi:10.1016/j.cell.2024.05.001.
660 46. Yue-Jie X, Cai-Zhi L, Ying C, et al. Glucocorticoids trigger muscle-liver crosstalk to attenuate
661 acute liver injury and promote liver regeneration via the FGF6-FGFBP1 axis[J]. *Mil Med*
662 *Res*. (2025) 12(1):36. doi:10.1186/s40779-025-00618-y.
663 47. Qian L, Sudan Z, Jiaren Z, et al. Colonic epithelial-derived FGF1 drives intestinal stem cell
664 commitment toward goblet cells to suppress inflammatory bowel disease[J]. *Nat Commun*. (2025)
665 16(1):3264. doi:10.1038/s41467-025-58644-2.
666

Supplementary Files

This is a list of supplementary files associated with this preprint. Click to download.

- file.pdf
- 3.supplementaryfileFig6WBGAPDH.tif
- 2.supplementaryfileFig6WBFGFBP1.tif
- 1.supplementaryfile1Fig6WBALDH1L1.tif
- 4.supplementaryfileFig2WBSyndecan1.tif
- 5.supplementaryfileFig2WBTNF.tif
- 5.supplementaryfileFig2WBTNF.tif